Biologically induced phosphorus precipitation in aerobic granular sludge process

Angela Manas, Biscans Beatrice, Mathieu Sperandio

Biologically induced phosphorus precipitation in aerobic granular sludge process

Mañas Angela [a,b,c,d], Biscans Béatrice [a,b,c,d], Spérandio Mathieu [a,b,c,*]

[a] Université de Toulouse, INSA, UPS, INP, LISBP, 135 Avenue de Rangueil, F-31077 Toulouse, France
[b] INRA, UMR792 Ingénierie des Systèmes Biologiques et des Procédés, F-31400 Toulouse, France
[c] CNRS, UMR5504, F-31400 Toulouse, France
[d] CNRS, UMR5503, 4, allée Emile Monso BP 84234-F-31432 Toulouse Cedex 4, France

ABSTRACT

Aerobic granular sludge is a promising process for nutrient removal in wastewater treatment. In this work, for the first time, biologically induced precipitation of phosphorus as hydroxyl-apatite ($Ca_5(PO_4)_3(OH)$) in the core of granules is demonstrated by direct spectral and optical analysis: Raman spectroscopy, Energy dispersive X-ray (EDX) coupled with Scanning Electron Microscopy (SEM), and X-ray diffraction analysis are performed simultaneously on aerobic granules cultivated in a batch airlift reactor for 500 days. Results reveal the presence of mineral clusters in the core of granules, concentrating all the calcium and considerable amounts of phosphorus. Hydroxyapatite appears as the major mineral, whereas other minor minerals could be transiently produced but not appreciably accumulated. Biologically induced precipitation was responsible for 45% of the overall P removal in the operating conditions tested, with pH varying from 7.8 to 8.8. Major factors influencing this phenomenon (pH, anaerobic phosphate release, nitrification denitrification) need to be investigated as it is an interesting way to immobilize phosphorus in a stable and valuable product.

1. Introduction

Phosphorous is a key nutriment for the development of life, constituting one of the major nutrients necessary for agricultural activity. However, the quantities of mineral phosphorus resources (phosphate rock) are decreasing in the world, making phosphorus recovery necessary in the coming century. On the other hand, the high phosphorus and nitrogen content of wastewaters leads to serious problems of eutrophication in ponds, rivers and seas. Therefore, research is now focusing increasingly on combined processes that remove phosphorous from wastewaters and simultaneously recover it in the form of a valuable product, for example, struvite or hydroxyapatite (De-Bashan and Bashan, 2004; Shu et al., 2006; Suzuki et al., 2006). Phosphorous recovery techniques are particularly suited to high strength wastewaters produced by anaerobic sludge digestion (Demirel et al., 2005; Lemaire, 2007). Calcium or magnesium phosphates can be formed by crystallization and recovered in specific reactors via pH control and chemical dosing (Seckler et al., 1996; Katsuura et al., 1998; Münch and Barrm, 2001; Giesen, 1999; Baur et al., 2008). The spontaneous phenomenon has been reported to cause economic damage related to pipe clogging when it is not controlled (van Rensburg et al., 2003). In activated sludge systems, biologically induced

phosphate precipitation has also been reported but less investigated (Maurer et al., 1999; Pambrun, 2005; De Kreuk et al., 2005). Calcium phosphate precipitation is thought to contribute to P removal in Enhanced Biological Phosphorous Removal processes (EBPR) and it is considered to enhance biological P removal efficiency (Maurer et al., 1999). Local precipitation is naturally induced when the pH and ion concentrations lead to mineral supersaturation. In the case of calcium or magnesium phosphate, their formation can be caused by phosphate release due to Polyphosphate Accumulating Organisms (PAO) during the anaerobic phase, but also clearly depends on pH. Bioreactions (e.g. nitrification and denitrification) or aeration (CO_2 stripping) lead to pH gradients which can be responsible for mineral precipitation in biological sludge (Pambrun, 2005; Bogaert et al., 1997; Saidou et al., 2009; Zhu et al., 2007). These processes still need to be clarified in granular sludge systems.

The aerobic granular sludge process is a promising technology for wastewater treatment because of its small footprint and capacity to treat high organic loading rates and its simultaneous nutrient removal through nitrification, denitrification and BioP accumulating processes (Morgenroth et al., 1997; Etterer and Wilderer, 2001; De Kreuk et al., 2005; Lemaire, 2007). The dense-spherical structure of granules leads to transfer limitations (Liu and Tay, 2004; Adav et al., 2008), promoting not only DO gradients but also local pH gradients coming from biological reactions, especially in the case of enhanced denitrification (Wan and Sperandio, 2009; Wan et al., 2009). As phosphate accumulating bacteria can also be present inside the granules (Lemaire, 2007), anaerobic phosphate release can encourage P precipitation within the core of the microorganisms, where subsequent solubilization of the crystals would be more difficult than in the bulk. Phosphate precipitation in a granular sludge process was assumed (but not directly demonstrated) by Yilmaz et al. (2007), De Kreuk et al. (2005) and De Kreuk and van Loosdrech (2007). By estimating its supersaturation index, Yilmaz et al. (2007) suggested that struvite could be transiently formed during the anaerobic phase of the SBR cycle. The contribution of this process to overall P removal was estimated to be less than 10 percent on the basis of a perchloric acid extraction method (Haas et al., 1988; Daumer et al., 2008). Similarly, experimental results by De Kreuk et al. (2005) suggest that P-removal occurs partly by biologically induced

precipitation in granular sludge. Extraction techniques indicated that 2.6% of the sludge mass was due to precipitates (P/VSS), but the whole contribution of this process compared to biological P removal processes was not quantified. For simplicity, precipitation was not included when modelling the process but De Kreuk and van Loosdrech (2007) proposed to increase the maximum fraction of polyphosphate in PAO from 0.35 (Hu et al., 2002) to 0.65 assuming that about 46% of the P removal could be due to P precipitation and 54% due to polyphosphate accumulating bacteria. Recently, Maurer et al. (1999) have proposed a model for naturally induced P precipitation in activated sludge, which is based on the assumption that hydroxyapatite (HAP) and hydroxydicalcium phosphate (HDP) are formed. The model can predict calcium and phosphate concentrations at different pH. However, in all these studies, phosphate minerals formed in biological granules or flocs have never been directly characterized, and the nature of the phosphate precipitate is not demonstrated but only indirectly deduced from stoichiometry of soluble species.

The characterization of precipitates inside aerobic granules is still a relatively unexplored field. Minerals involved in phosphorus immobilization have been poorly qualified in biological sludge because traditional techniques (like X-ray diffraction) are difficult to apply directly in such organic matrices (Cloete and Oosthuizen, 2001). SEM-EDX analysis has recently been applied to determine calcite formations in granules and in nacre shells (Ren et al., 2008). However, calcium or magnesium phosphates have not been quantified in previous studies of aerobic granules (Wang et al., 2006; Ren et al., 2008).

Therefore, the aim of this study is to reveal the nature of P minerals which can accumulate in EBPR granular sludge systems. In an attempt to determine the chemical composition of precipitates in granules, RAMAN spectroscopy, EDX (Energy Dispersive X-ray) technique coupled with Scanning Electron Microscopy (SEM), and X-ray Diffraction analysis (XRD) are evaluated.

2. Materials and methods

2.1. Reactor operating conditions

Aerobic granules were cultivated in a Sequencing Airlift Batch Reactor (SBAR), with a working volume of 17 L, consisting of an

airlift column (D = 15 cm, H/D ratio = 7) with a baffle plate (length/width = 83/15-cm-). An aerating diffuser providing fine bubbles 3 mm in diameter was inserted at the bottom of the reactor at one side of the baffle plate, achieving mixing during both anoxic and aerobic phases (using nitrogen gas for the anoxic phase and air for the aerobic one). Oxygen concentration and pH were measured and recorded online with selective probes (WTW TriOxmatic 701). Temperature was maintained constant at 20 °C thanks to a water jacket. Details of the system schematization can be seen in Wan, 2009. Process batch cycles of 4 h length were established as follows: anoxic phase (20 min), aerobic reaction (145 min), idle (30 min), withdraw (30 min) and feed (15 min). Hydraulic Retention Time (HRT) was fixed at 8.5 h, with a volumetric exchange ratio of 50%. The column was fed at the bottom with a synthetic substrate (details in Wan et al., 2009) having the following composition: COD of 1000 mg/L (25% contribution each of glucose, acetate, propionic acid and ethanol); $[PO_4^{3-}]$ = 30 mgP/L, $[Ca^{2+}]$ = 46 mg/L, $[HCO_3^-]$ = 100 mg/L, $[MgSO_4 \cdot 7H_2O]$ = 12 mg/L, $[NH_4^+]$ = 50 mgN/L, $[NO_3^-]$ = 100 mgN/L. Therefore, a COD/N$-$NH$_4^+$ ratio of 20 was maintained, and nitrate was dosed in order to maintain an anoxic phase after feeding. Influent loading rates coming into the reactor were as follows: 0.14 gN L^{-1} d^{-1} for ammonium, 0.08 gP L^{-1} d^{-1} for ortho-phosphate and 2.82 gCOD L^{-1} d^{-1} for organic substrate.

2.2. Analytical characterization of the liquid and solid phases

Chemical analyses were conducted according to standard methods (AFNOR, 1994). COD (NFT 90-101), MLSS (NFT 90-105) and MLVSS (NFT 90-106). NO_2^-, NO_3^-, PO_4^{3-}, NH_4^+, Ca^{2+}, K^+, Mg^{2+} concentrations were analyzed by Ion Chromatography (NFT 90-023) after being filtered with 0.2 μm pore-size acetate filters. Microscopic observations over the whole sludge sample were performed with a Biomed-Litz® binocular photonic microscope. Particle size distribution was measured with a Malvern 2000 Mastersizer® analyser. Granules were sampled at the end of the aerobic phase. Those analyzed by EDX or Raman Spectroscopy had been previously cut into thin slices of 100 μm using a cryo-microtome (Leica CM 30505 Kryostat). Those analysed by XRD had been previously dried and calcined in an oven at 500 °C for 2 h, in order to remove the organic fraction.

Raman Spectroscopy was performed with an RXN Kaiser Optical Systems INC at a wavelength of 785 nm in the visible range. Two different optical fibres were used for the incident (50 μm) and collected (100 μm) rays. EDX analysis was performed with a photon X analyzer (Quantax Technology Silicon Drift) having a detection limit of 127 eV. It was coupled to a SEM (JEOL 5410 LV) which allowed working in a partial pressure chamber. The reference samples used for comparing the mineral spectra were: struvite (CAS N.13478-16-5), calcite (CAS N. 72608-12-9), magnesite (CAS N. 235-192-7), hydroxy-apatite (CAS N. 12167-74-7) and brushite (CAS N. 7789-77-7).

XRD analyses were performed with a BRUCKER D5000 diffractometer, with a cobalt tube scattering from 4 to 70° in 2θ.

Chemical nitrogen and total phosphorus extractions were performed in accordance with standard methods (NFT 90-110

and NFT 90-136 respectively) adapted for the granular samples: first a physical separation was made between flocs and granules by means of a 315 μm shiver, then granules were rinsed with a volume of ultrapure water and the volume of sample extracted was re-established with ultrapure water before analysis.

The Supersaturation Index (SI) for each mineral considered (eq. (1)) was calculated as the logarithm of supersaturation ratio:

$$SI = \log \Omega = \log \left(\frac{IAP}{[K']} \right)^{1/j} \tag{1}$$

where IAP is the Ionic Activity Product of the ion concentrations involved in the mineral precipitation; j is the number of ions of the mineral and K' refers to the conditional solubility product, which includes the thermodynamic mineral precipitation constant at a given temperature, the ionic activity coefficients, and the ionization fractions of each component (Snoeyink and Jenkins, 1980; Burriel et al., 1985). The PHREEQC software (Minteq.v4 database) was used to calculate the chemical equilibrium for each sample collected in the reactor. Ionic Strength was taken into account as well as the ionic activity coefficients by the Davies approach (Parkhurst et al., 1980; Burriel et al., 1985; Mostastruc, 2003). pKp of struvite (STR), hydroxyapatite (HAP), brushite (DCPD), amorphous calcium phosphate (ACP) and hydroxyl dicalcium phosphate (HDP) considered were respectively: 13.26, 57.5, 6.6, 26.52 and 22.6 (Ohlinger et al., 1998). Oversaturating conditions were considered to be achieved when SI > 0.5 (theoretically zero but a security margin is usually given (Burriel et al., 1985; Rahman et al., 2006)).

3. Results

3.1. Reactor performance and kinetics assessment

The sequencing batch reactor was operated for 540 days. Mean efficiencies of COD, total Nitrogen and Phosphorous removal, as well as MLSS, MLVSS and SVI$_{30}$ values are shown in Table 1. An SVI$_5$/SVI$_{30}$ ratio closer to 1, indicates a major presence of granules in the whole sludge. MLVSS and MLSS of the whole sludge were measured regularly in the reactor with

Table 1 — Mean values measured during 500 days of reactor performance, for Mixed Liquor Suspended Solids; soluble COD, Total Nitrogen and Phosphorous efficiencies; MLVSS/MLSS ratio, Sludge Volume Index after 30 min and SVI$_5$/SVI$_{30}$ ratio.

Period of time (days)	MLSS (g/L)	η COD (%)	η TN (%)	η P (%)	MLVSS/ MLSS —	SVI$_{30}$ (mL/g)	SVI$_5$/ SVI$_{30}$ —
0−100	14	94	92	62	78	33	2.0
100−200	13	97	100	31	83	34	1.7
200−300	22	93	96	56	77	22	1.5
300−400	28	93	96	67	67	15	1.0
400−500	34	97	97	50	65	15	1.0
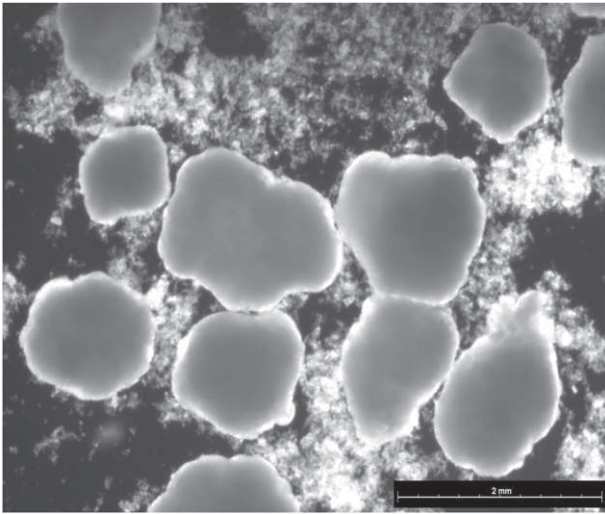
Fig. 1 – Granules and flocs in the reactor after 520 days of operation. The bar dimension is 2 mm.

time, values of 30–35 and 21–25 g/L being achieved for MLSS and MLVSS respectively at the end of the study. The MLVSS/MLSS ratio of granules progressively decreased from 80% to 67%, indicating mineral accumulation. Final SVI_5 was 15 mL/g. As shown in Fig. 1, the mixed liquor in the reactor was composed of granules and flocs, the latter disappearing progressively with time. Particle size distribution analyses revealed that 800 μm was the most probable diameter for granules. At the end of the 540 days of reactor run, removal efficiencies achieved were 100% for ammonium, 100% for nitrate, 82% for ortho-phosphates and 99% for soluble COD.

Kinetic analyses were performed during the batch cycle to assess ammonia, nitrate, COD and phosphate removal rates. Figs. 2 and 3 show typ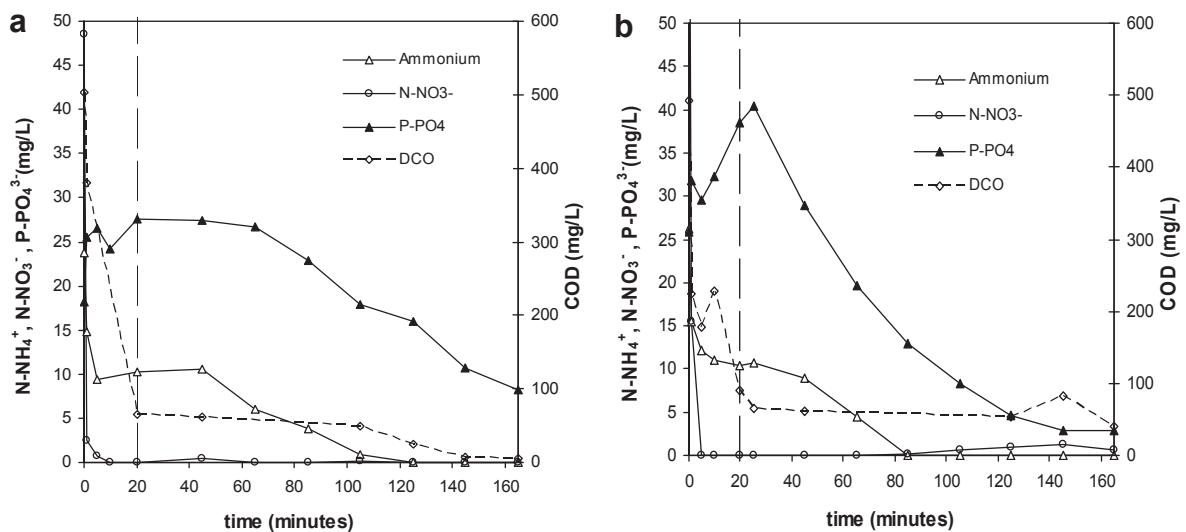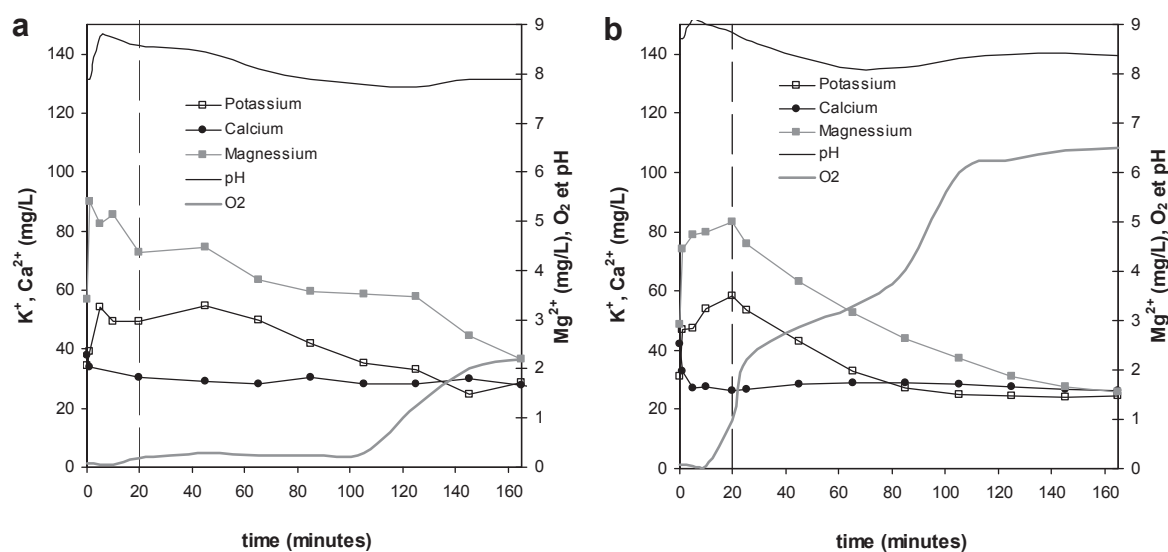ical time-series profiles in the reactor obtained with two different aeration flow rates (160 L/h and 350 L/h respectively). The separation between the anoxic/aerobic phases is depicted by a dotted vertical line.

Ammonium was first partially removed during the non-aerated phase and then during the aerobic phase via nitrification. Ammonium consumption during the anoxic phase was due to heterotrophic assimilation but it could also be explained by other, non-biotic processes like adsorption (because of high MLSS) or precipitation (as struvite for example). Nitrate and nitrite concentration remained negligible at all times, confirming that simultaneous nitrification and denitrification occurs in granular sludge. Regarding phosphorus, several mechanisms seemed to take place simultaneously. Kinetics in Figs. 2 and 3, show phosphorus release during the anaerobic phase and P uptake during the aerobic period, Meanwhile, biological staining with sudan black and safranin was carried out according to the method reported in Pandolfi et al. (2007), revealing lipid and PHB accumulations in different granules samples taken during the anoxic phase (results not here shown). Both kinetics and color staining results, suggested the presence and activity of Poly-phosphate Accumulating Organisms (PAO). Fig. 2a and b show that phosphate uptake rate was higher for higher aeration rate, because dissolved oxygen was limiting at low aeration rate (DO being maintained at 0.3 mg/L). Final phosphate concentration was thus lower at the high air flow rate (2.5 mgP/L) compared to the low aeration rate (8 mgP/L). Mg^{2+} and K^+ fluctuations followed those of P (Fig. 3a and b). This was related to polyphosphate synthesis, which general formula is $Me_{n+2}P_nO_{3n+1}$, where n indicates the chain length, and Me represents a metal cation (Jardin and Pöpel, 1996). In contrast, Ca^{2+} concentration showed a very different trend. It decreased rapidly during the non-aerated period following wastewater feeding. This behavior can be explained by a rapid formation of calcium complexes or precipitates, which will be demonstrated in the following section.

Total phosphorus was extracted from granular sludge samples collected at the end of the aerobic cycle. It was carried out in triplicate after 520 days of reactor operation (according to the method detailed in section 2.2). Results indicated that P content was 56 ± 7.3 mgP/gSS. This value is not really different from values usually reported for EBPR sludge. In EBPR

Fig. 2 – Variation of NO_3^-, PO_4^{3-}, NH_4^+ and COD in the reactor bulk during a cycle operation with weak aeration (160 L/h) (2a) and high aeration (350 L/h) (2b) rates.

Fig. 3 – Variation of K^+, Mg^{2+}, Ca^{2+}, pH and O_2 in the reactor bulk during a cycle operation with weak aeration (160 L/h) (3a) and high aeration (350 L/h) (3b) rates.

systems, this value is related to the polyphosphate content of sludge, which depends on various parameters: fraction of PAO in the sludge, wastewater COD/P ratio and fraction of volatile fatty acids in wastewater. Li and Liu (2005) reported a similar P content at a similar P/COD ratio. However, the following paragraph will show that phosphorus is not only accumulated in polyphosphate form but also as a precipitated mineral compound.

3.2. Raman analysis

Raman analysis is a non-destructive analytical technique that requires limited sample preparation (Hollas, 1996; Skoog and Nieman, 2003). It was chosen because of its low water background, as well as for providing sharper and clearer bands than IR spectra (Barbillat, 2009). It has already been proved for the characterization and identification of different biological systems since the biologically associated molecules can exhibit a unique spectral pattern (Ivleva et al., 2009). In an attempt to determine the internal structure of the granules, samples were cut into slices of 100 μm width, prepared as described in section (2.2). Then, a central slice was chosen and observed with a binocular microscope before being analyzed by Raman Spectroscopy. As shown in Fig. 4a, microscopic observation of a typical central slice revealed a white crystalline precipitate in the centre of the granule. Spectroscopic analysis was performed at different points of the mineral core (as indicated on Fig. 4a). An initial set of tests (not shown) was also conducted beforehand with different samples: granules taken at different batch cycle times, dehydrated flocs separately, different cuts and thicknesses sliced from the same granule. Finally, some pure minerals used as reference products (Struvite, hydroxyapatite, brushite, calcite and magnesite), were also analyzed with Raman Microscopy and compared to the sample spectra. The following conclusions were drawn: (i) Both flocs and external granule slices showed irregular curved spectra (due to organic matter) with no

remarkable matching peaks (ii) All spectra obtained in the core of granules showed a common and reproducible pattern of 8 peaks of different intensities (see Fig. 4b), considering that a peak is noted when its intensity is three times the mean background noise; (iii) All granule central slices had the same typical peaks regardless of the cycle time.

According to Fig. 4b, the most important peaks in the sample were found at the following Raman shifts (cm^{-1}): 430, 588, 850, 962, 1072, 1135, 1295, 1448.

The spectra of granule core samples were compared with those obtained with reference minerals. After an individual comparison of frequency-intensity coincidence, it was concluded that calcite and magnesite spectra (not shown) did not match the sample at all. In Fig. 5, the most similar mineral spectra have been depicted in order to compare the coincidence of their peaks. Brushite shows two or three peaks not far from those of granule spectra, but most of the major peaks do not coincide (407, 586, 986, 1056 and 1114 cm^{-1}). Struvite spectrum indicates five peaks (421, 563, 944, 1053, 1112 cm^{-1}) which are very similar to those of the granule sample, but differences in the Raman shifts are statistically significant. The hydroxyapatite spectra show 4 peaks, which all match the granule spectra (427, 589, 962, 1072 cm^{-1}) with differences lower than 3 cm^{-1}. Globally, among all the different pure mineral patterns compared, the hydroxyapatite spectrum best fitted the sample in intensity and wave number but could not explain all the peaks observed in the granule spectra. These results suggest that hydroxyapatite is a major mineral precipitated in the aerobic granule cores but the presence of other minerals cannot be totally discounted.

3.3. SEM-EDX analysis

Scanning Electron Microscopy (SEM) coupled with Energy Dispersive X-ray detector (EDX) analyses were carried out on cut mature granules. Typical images are shown in Fig. 6 for two typical central slices of different granules. It was
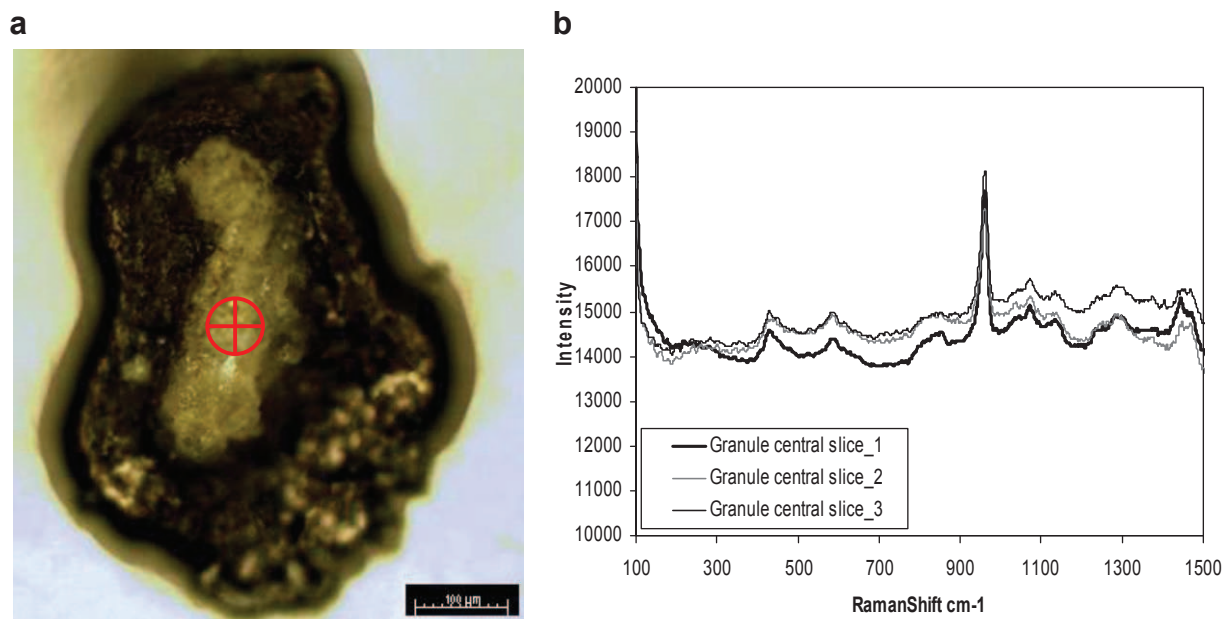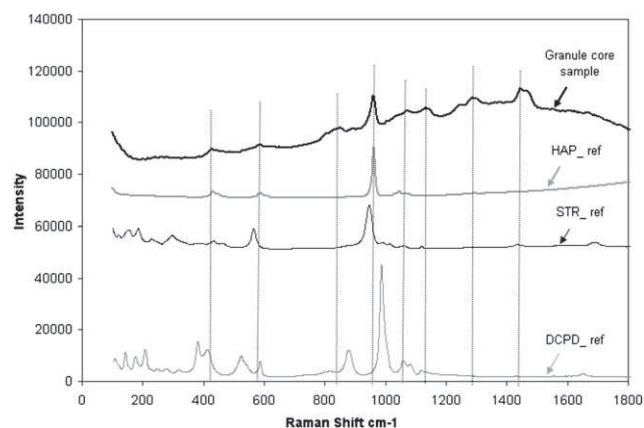
Fig. 4 – a: Central slice from a mature granule after 450 days of reactor run. The bar length is 100 μm. b: Spectra of core aerobic granule slices.

found that inorganic precipitates occupied an important fraction of the total volume of the granule, located in different zones, mainly close to the centre. A first scanning map of carbon (Fig. 6c and d) revealed that the central inorganic zones did not contain large amounts of carbon in contrast with peripheral organic biofilm. Similar results were observed for nitrogen and magnesium (not shown). In contrast Ca and P were mainly found together in the central precipitates and comparatively poorly in the organic biofilm (Fig. 6e−h). This result again supports the idea that calcium phosphates are formed in the core of the granules. Phosphorus was also detected but with lower concentration in the organic biofilm zone. It probably came from polyphosphates in PAO clusters. Fig. 6i and j, focus on the inorganic precipitate with a higher objective. Fig. 6i reveals porous, ordered holes in the solid mineral phase. This could be related to the mechanism of

precipitate formation around bacterial cells, in relation with gaseous transfers between the microorganisms and the extracellular medium. Another interesting result can be seen in Fig. 8j, where some prismatic structures appear stacked, similar to hydroxyapatite, which crystallizes in the hexagonal system (Morgan et al., 2000;). Furthermore, several localized EDX spectral analyses were made, pointing the probe at different locations of the precipitate. The spectrum obtained was very reproducible in different locations of the central mineral zone (Fig. 6k). Analysis spectra clearly showed that calcium, phosphate and oxygen were the major components observed in the mineral zone whereas magnesium and potassium were definitively absent. Quantitative analysis over 5 different samples showed that the Ca/P mean atomic ratio obtained for the mineral precipitate was 1.63 ± 0.05, which is quite close to the theoretical one for hydroxyapatite (1.67).

In parallel, scanning analyses of the flocs and supernatant (not shown) did not reveal any similar calcium phosphates but some sparse mineral particles with high K, Mg and P content were found. These analyses indicated that calcium phosphates were exclusively accumulated in the granules whereas other minerals could be formed in the bulk, e.g. magnesium phosphate, ammonium struvite ($MgNH_4PO_4 \cdot 6H_2O$) or potassium struvite ($KMgPO_4 \cdot 6H_2O$). However, they were detected in much smaller amounts than hydroxyapatite.

3.4. XRD analysis

XRD analysis is an efficient tool for distinguishing crystalline minerals from those of amorphous structure, so it was also carried out on some granule samples. Three different preparations of granular samples were tested. Results of two sample analyses (not shown), i.e. a sample of dried pulverised granules and a wet sludge sample, revealed a major peak

Fig. 5 – Spectra of reference minerals compared to a granule central slice.

The EDX spectrum in Fig. 6k:

Spectrum: 0 3

Element	Series	norm. C [wt.%]	Atom. C [at.%]
azote	K-series	0.00	0.00
phosphore	K-series	12.87	**8.77**
oxygène	K-series	56.33	74.31
magnésium	K-series	0.89	0.78
calcium	K-series	28.75	**15.14**
sodium	K-series	0.95	0.87
soufre	K-series	0.20	0.13
	Total:	100.00	100.00
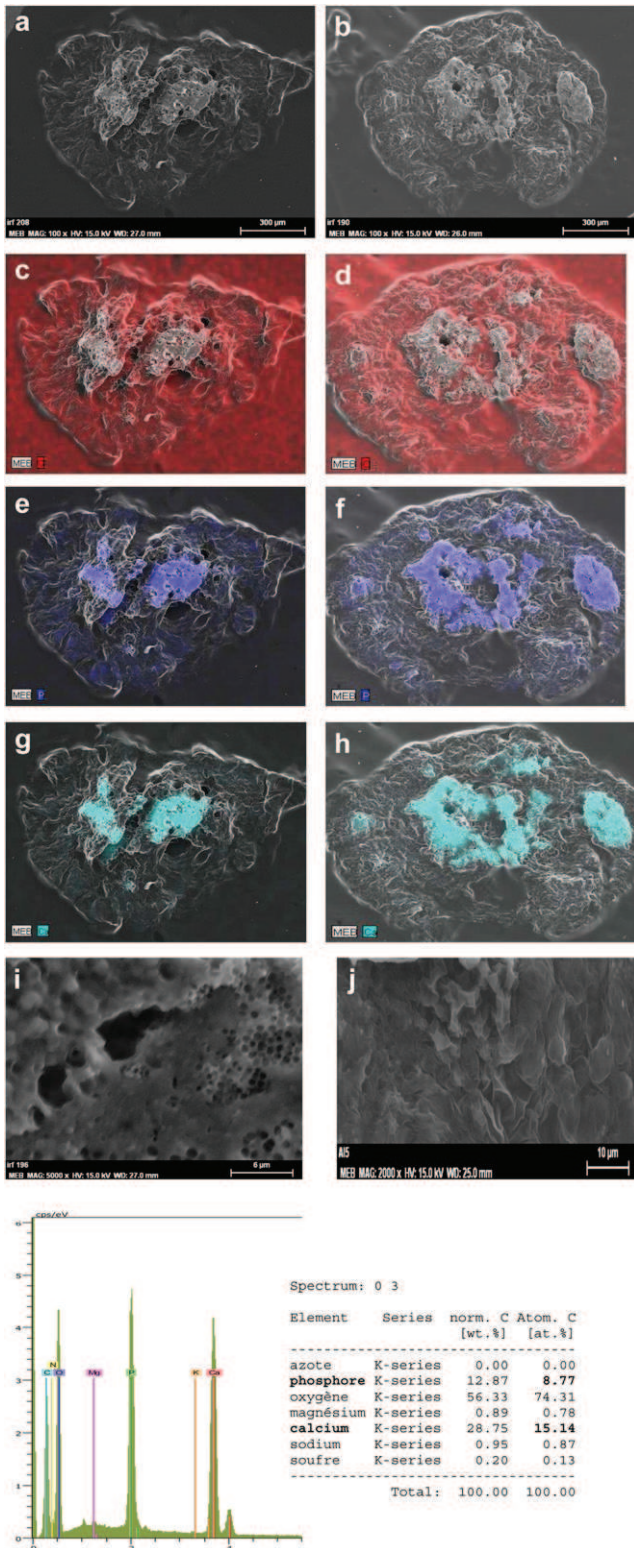
Fig. 6 − a: SEM image of a granule central slice. b: SEM image of a granule central slice. c: Carbon (red) scanning with EDX. d: Carbon (red) scanning with EDX. e: P (dark blue) scanning with EDX. f: P (dark blue) scanning with EDX. g: Ca (light blue) scanning with EDX. h: Ca (light blue) scanning with EDX. i: granule precipitate SEM images. j: granule precipitate SEM images. k: Punctual analysis with EDX probe of a precipitate grown in a biological granule. (For interpretation of the references to colour in this figure legend, the reader is referred to the web version of this article.)

coinciding with calcium phosphate patterns. However, high noise due to the organic fraction was present, making any interpretation difficult. Thus, a third granular sludge sample was treated to remove the organic matter (described in 2.2), leading to the diffractogram presented in Fig. 7. A number of distinct rays indicate the presence of crystalline forms. By comparison with reference spectra, most of the peaks, and in particular the bigger ones, coincided with those of the hydroxyapatite spectrum ($Ca_5(PO4)_3(OH)$). The remaining minor peaks coincided with whitlockite ($Ca_{18}Mg_2H_2(PO_4)_{14}$). The large central peaks indicate the possible presence of amorphous mineral species.

It should not be forgotten that, for XRD analysis, the sample was heated to 500 °C and so some hydroxylation phenomena could have taken place. Considering that hydroxyapatite dehydroxilation does not occur under 800 °C (Wang et al., 2004), changes of this mineral in the original sample, due to heating, would not take place. However, in the range of 200−400 °C, dehydratation of the lattice and adsorbed water of some other minerals could be possible according to Kohutova et al. (2010). The magnesium and phosphorus initially present in organic polymers (polyphosphate) could precipitate in a new form during heating. Despite the fact that XRD again confirmed the major formation of hydroxyapatite, it is still difficult to know whether other intermediates were present or not and, in the case of whitlockite (WHT), it might have been formed during the heating process.

4. Discussion

4.1. *Hydroxyapatite: a major phosphate mineral in aerobic granules*

All the results (Raman spectroscopy, SEM-EDX, and XRD) support the same conclusion: hydroxyapatite (HAP) was the major mineral found inside the phosphorus-rich granules in this study. Both Raman and SEM-EDX analysis allowed calcium phosphate mineral to be identified and XRD analysis confirmed its crystalline form, but also suggested the presence of other amorphous minerals. SEM-EDX analysis in Fig. 6e and f, pointed out that P was also present in the organic fraction of the aggregates, probably linked to polyphosphate stored in bacterial biofilm. This last statement may be supported by the fact that Mg and K elements, which are linked to polyphosphate constitution, were also found sparsely in this area. SEM-EDX indicates a very reproducible Ca/P ratio (1.63 ± 0.05) coinciding with that of hydroxyapatite (1.67), and notably different from other calcium phosphates (e.g. amorphous calcium phosphate: 1.50; hydroxydicalcium phosphate: 2; whitlockite: 1.3). XRD analysis finally confirmed the presence of crystalline hydroxyapatite, possibly associated with amorphous forms. Considering that most of the calcium was immobilized with phosphorus (as indicated by SEM-EDX images) with a Ca/P ratio
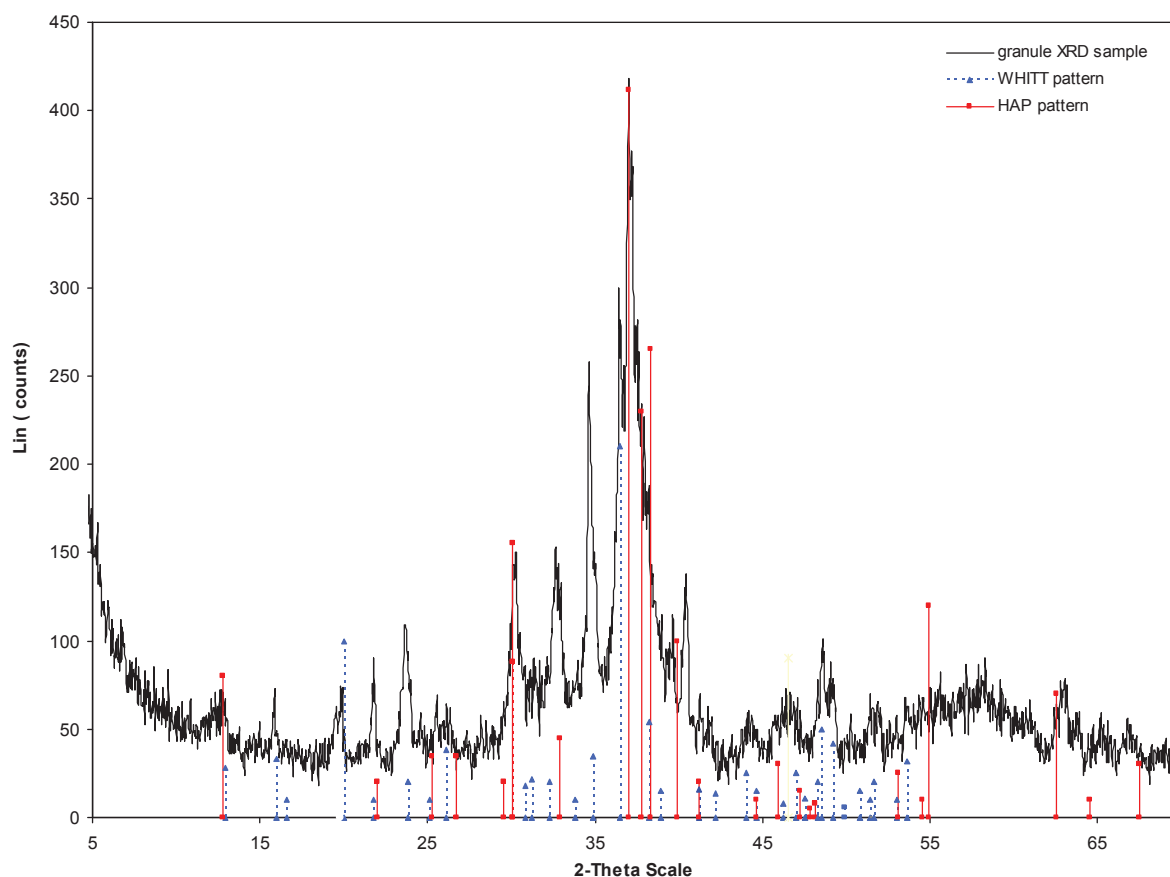
**Fig. 7 – XRD diffractogram of a granule sample compared to HAP and WHT pattern.**

of 1.67 (hydroxyapatite), it is possible to estimate the contribution of precipitation to global P removal. As Ca^{2+} removal yield of 46% was obtained (0.488 mmol/L), it means that about 0.292 mmolP/L was removed via hydroxyapatite precipitation. This represents about 45% of the total P removal in the process (82% of P was removed which represents 0.68 mmol/L), the rest being explained by biological mechanisms. The precipitation contribution is hence much more significant than those estimated in flocculated sludge (Haas et al., 1988). But this is in accordance with the data obtained with granular sludge by De Kreuk et al. (2005) and De Kreuk and van Loosedrech (2007), which suggest that P accumulation in EBPR granules can double the accumulation achieved in flocs, because of precipitation.

In the calcium phosphate family, hydroxyapatite (HAP) is commonly considered as the most stable phase and the most insoluble one. According to Ostwald's ripening theory (Mullen et al., 2001), precursors such as brushite (DCPD), octacalcium phosphate (OCP), and amorphous calcium phosphate (ACP) contribute to its formation, brushite being the most soluble phase. Hydroxyapatite and brushite were both considered in this study as reference samples but brushite was not detected (Raman). In one sense, our results confirm the first assumption of Maurer et al. (1999) who supposed that hydroxyapatite can be accumulated in EBPR systems. However Maurer et al. (1999) also supposed that HDP was formed as an intermediate without any convincing explanation for that choice, and this assumption is difficult to confirm in our case.

Of all the minerals that could be found in wastewater treatment (Musvoto et al., 2000; van Rensburg et al., 2003; Larsdotter et al., 2007), only a few were expected to precipitate in granular sludge, in particular calcium carbonate (Ren et al., 2008; Wang et al., 2006), or struvite (Yilmaz et al., 2007). Calcium carbonate in calcite form, was previously detected in biological aggregates and aerobic granules (Ren et al., 2008; Wang et al., 2006). Due to their competition for calcium (Lin and Singer, 2006) mineral phosphate and carbonate can inhibit each other. According to several authors (Montastruc et al., 2003; Bellier et al., 2006), pH plays an important role, favouring phosphate precipitation at pH 7–8.5, whereas both carbonates and phosphates co-precipitate at pH 9–11. In our case, absence of calcite could be explained simultaneously by low calcium availability due to hydroxyapatite formation and inappropriate pH inside the granules. In contrast with the assumption of Yilmaz et al. (2007), no struvite was detected in the granules and struvite precipitation seems to have played a minor role in phosphate immobilisation in our study. However, samples were taken at the end of the aerobic period, and it is possible that struvite had been transiently formed in the previous anaerobic phase and afterwards solubilized as ammonia was consumed during nitrification.

4.2. Parameters controlling phosphorus precipitation in EBPR granular sludge

Supersaturation index calculation (SI) for different minerals, for the supernatant, established for each time of the kinetic
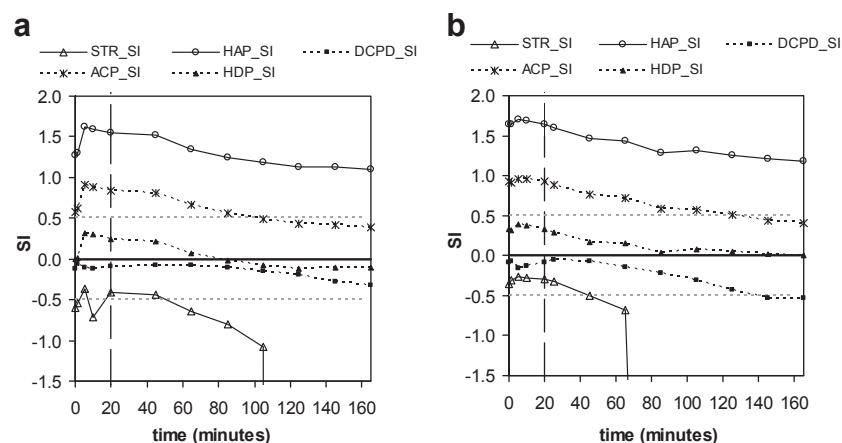
Fig. 8 — a: Saturation Index for several minerals in the bulk during a cycle with weak aerating conditions. b: Saturation Index for several minerals in the bulk during a cycle with strong aerating conditions.

experiments are shown on Fig. 8. Saturation index was calculated using the Minteq.v4 database (PHREEQC, software) with the pH and concentrations measured in the bulk. Struvite saturation index was negative throughout the batch cycle and lessened progressively with ammonia consumption by nitrification. This indicates that the ammonium and magnesium concentrations were too low to cause struvite precipitation in those conditions. Concerning calcium phosphates, the saturation index for brushite and hydroxydicalcium phosphate were close to zero, i.e. these minerals were not considerably oversaturated. This suggests that the latter were poorly or very briefly formed, only during the feeding period. SI for amorphous calcium phosphate varied from around 1 to less than 0.5. Finally, the highest value of SI (from 1.7 to 1.2) was obtained for hydroxyapatite, i.e. the most stable phase among the calcium phosphates showed oversaturation conditions throughout the experiment.

In addition, for all the compounds studied, SI decreased during the aerobic phase, because phosphate concentration lessened (due to P uptake) and pH decreased (due to nitrification). This result confirms that precipitation of calcium phosphate is more probable during the initial anoxic period, which is in accordance with the tendency observed for calcium (Fig. 3).

Additionally, hydroxyapatite precipitate was observed in the core of granules. This means that confined conditions were more favorable for hydroxyapatite formation or accumulation than conditions in the bulk. Three explanations can be proposed: (1) higher local phosphate concentration, (2) higher local pH and (3) higher retention time for granules.

Firstly higher local phosphate concentration is probably reached during the anaerobic period due to phosphate release by PAO in the internal part of granules. Simultaneously, calcium was also provided during the anaerobic period by means of wastewater feeding. In parallel, observed phosphate release was relatively moderate and would probably have been more significant if precipitation had not occurred. This shows that feeding anaerobically is a method that encourages P precipitation. Secondly, pH is obviously an important parameter controlling phosphate precipitation (high pH increases hydroxyapatite supersaturation). Therefore, another possible

explanation for hydroxyapatite accumulation in the core of granules is the fact that internal pH can be higher than bulk pH, because of denitrification. A last mechanism is the fact that high retention time of granules encourages the formation of the most stable calcium phosphate (HAP) due to low formation rate and low solubilization rate, whereas other calcium phosphates mentioned before can be transiently produced and resolubilized.

More generally, the importance of calcium precipitate depends on influent characteristics. In this work, the range of phosphate concentration was similar to those explored by Maurer et al. (1999). It was slightly higher than those found in conventional domestic wastewater but lower than those reported for high strength wastewater like agro-food industry waste (Yilmaz et al., 2007). Calcium, magnesium, and ammonium concentrations were at moderate levels, similar to those found in domestic wastewater. Comparatively to other studies, pH was relatively high in this work, ranging from 7.8 to 8.8 in a typical SBR cycle. This was due either to bicarbonate stripping (pH was higher at high flow rate) and denitrification, and hence, these two processes clearly encourage hydroxyapatite precipitation.

4.3. Advantage of hydroxyapatite accumulation in granular sludge

Hydroxyapatite is a phosphorus compound that is much more stable than bacterial polyphosphate. In EBR systems, sludge containing polyphosphates needs to be extracted and removed rapidly from the system in order to avoid problems with secondary P release. This makes it obligatory to restrict the sludge retention time to a reasonable value, and then anaerobic storage is impossible as phosphate would be released in the liquid phase. In contrast, hydroxyapatite accumulation is advantageous because long retention time for granules is possible, as well as storage before agricultural use. In addition, from our experience (data not presented), granules with a mineral HAP core are very stable and can be easily dehydrated.

Finally induced precipitation in granules seems to be completely compatible with biological reactions. In

comparison, one of the reported drawbacks of simultaneous phosphorus precipitation in activated sludge process with calcium (lime) is that precipitation occurs at high pH (e.g. 9), which would be out of the optimal pH range for most biological processes (Carlsson et al., 1997; Arvin, 1979). High reactant excess is also necessary to reach very low P concentration at conventional pH. In the Phostrip® process, lime addition is thus performed on a side stream anaerobic reactor (Brett et al., 1997). In contrast, due to important gradients within granules, it is possible to maintain conditions in the core (favourable for precipitation) which are different from those in the external zone. In contrast with previous experience with flocculated sludge, it is shown in this study that hydroxyapatite accumulation in granular sludge is perfectly compatible with major biological reactions. Future work will be necessary to find the practical conditions which allow advantage to be taken of this process during the treatment of real wastewater.

5. Conclusions

For the first time, different analyses (Raman, SEM-EDX, XRD) have revealed the nature of phosphorus precipitates in an EBPR granular sludge process.

- Raman analysis provided a repetitive pattern over a granule core sample. The four main peaks coincided with those of hydroxyapatite ($Ca_5(PO_4)_3(OH)$)
- SEM-EDX demonstrated the presence of mineral clusters in the core of granules. These clusters concentrated most of calcium and phosphorus and EDX revealed that Ca/P ratios (1.63 ± 0.05) were close to the ratio of hydroxyapatite.
- XRD analysis of the mineral fraction of the sludge confirmed that the major mineral present was a crystalline hydroxyapatite, although it probably coexists with other minor amorphous calcium phosphates.

This work reveals that hydroxyapatite accumulation is an important phenomenon in the EBPR granular sludge process and merits attention in the future. In the conditions tested, it is estimated that about 45% of the P removal was due to biologically induced precipitation. In that sense, future work should focus on the operating conditions which favor hydroxyapatite accumulation as it could become an interesting way of immobilizing and recycling phosphorus.

Acknowledgments

R E F E R E N C E S

Adav, S.S., Lee, D.-J., Show, K.-Y., Tay, J.-H., 2008. Aerobic granular sludge: recent advances. Biotechnology Advances 26 (5), 411–423.

Arvin, E., 1979. The influence of pH and calcium ions upon phosphorus transformations in biological wastewater treatment plants. Progress in Water Technology 1, 19–40.

Barbillat, 2009. Spectroscopie Raman. Techniques de l'ingénieur P2865–1.

Baur, R., Ram, Prasad, Ahren, Britton, 2008. Reducing ammonia and phosphorus recycle loads by struvite harvesting. Ostara Nutrient Recovery Processes Brochure for WEFTEC 2008.

Bellier, N., Chazarenc, F., Comeau, Y., 2006. Phosphorus removal from wastewater by mineral apatite. Water Research 40 (15), 2965–2972.

Bogaert, H., Vanderhasselt, A., Gearney, K., Yuan, Z., Thoeye, C., Verstraete, W., 1997. A new sensor based on pH effect of denitrification process. Journal of Environment Engineering 123, 884–891.

Brett, S., Guy, J., Morse, G.K., Lester, J.N., 1997. Phosphorus Removal and Recovery Technologies. Selper Publications, London.

Burriel, F., Lucena, F., Arribas, S., Hernández, J., 1985. Química Analítica Cualitativa, eighth ed. Ed. Thompson.

Carlsson, H., Aspegren, H., Lee, N., Hilmer, A., 1997. Calcium phosphate precipitation in biological phosphorus removal systems. Water Research 31 (5), 1047–1055.

Cloete, T.E., Oosthuizen, D.J., 2001. The role of extracellular polymers in the removal of phosphorous from activated sludge. Water Research 35 (15), 3595–3598.

Daumer, M.-L., Béline, F., Spérandio, M., Morel, C., 2008. Relevance of a perchloric acid extraction scheme to determine mineral and organic phosphorus in swine slurry. Bioresource Technology 99 (5), 1319–1324.

De Kreuk, M.K., van Loosdrech, 2007. Formation of aerobic granules with domestic sewage. Environment Engineering 132 (1), 694–697.

De Kreuk, M.K., Heijnen, J.J., Loosdrecht, Van, 2005. Simultaneous COD, nitrogen and phosphate removal by aerobic granular sludge. Biotechnology and Bioengineering 90 (6), 761–769.

De-Bashan, L.E., Bashan, Y., 2004. Recent advances in removing phosphorus from wastewater and its future use as fertilizer (1997–2003). Water Research 38 (19), 4222.

Demirel, B., Yenigun, O., Onay, T.T., 2005. Anaerobic treatment of dairy wastewaters: a review. Process Biochemistry 40 (8), 2583–2595.

Etterer, T., Wilderer, P.A., 2001. Generation and properties of aerobic granular sludge. Water Science and Technology 43 (3), 19–26.

Giesen, A., 1999. Crystallization Process enables environment friendly phosphate removal at low cost. Environmental Technology 20, 769–775.

Haas, D.W., Lötter, D.W., Dubery, I.A., 1988. An evaluation of the methods used for the determination of ortho-phosphate and total phosphate in activated sludge extracts. Water Science 15 (4), 257–260.

Hollas, J.M., (1996). Spectroscopy (3rd ed.). Ed. Dunod.

Hu, Z.-r., Wentzel, M.C., Ekama, G.A., 2002. Anoxic growth of phosphate-accumulating organisms (PAOs) in biological nutrient removal activated sludge systems. Water Research 36 (19), 4927–4937.

Ivleva, N.P., Wagner, M., Haisch, C., Niessner, R., Horn, H., 2009. Combined use of confocal laser scanning microscopy (CLSM) and Raman microscopy (RM): Investigations on EPS - Matrix. Water Research 43 (1), 63.

Jardin, N., Johannes Pöpel, H., 1996. Influence of the enhanced biological phosphorus removal on the waste activated sludge production. Water Science and Technology 34 (1–2), 17.

Katsuura, H., 1998. Phosphate recovery from sewage by granule forming process (full scale struvite recovery from a sewage works at Shimane Prefecture, Japan). In: International Conference on Phosphorus Recovery from Sewage and Animal Waste. Warwick University, UK.

Kohutova, A., Honcova, P., Podzemna, V., Bezdicka, P., Vecernikova, E., Louda, M., Seidel, J., 2010. Thermal analysis of kidney stones and their characterization. Journal of Thermal Analysis and Calorimetry 101 (2), 695–699.

Larsdotter, K., La Cour Jansen, J., Dalhammar, G., 2007. Biologically mediated phosphorus precipitation in wastewater treatment with microalgae. Environmental Technology 28 (953), 960.

Lemaire R. 2007. Development and fundamental investigations of innovative technologies for biological nutrient removal from abattoir wastewater. Ph.D Thesis. University of Queensland, Australia.

Li, Y., Liu, Y., 2005. Diffusion of substrate and oxygen in aerobic granule. Biochemical Engineering Journal 27 (1), 45–52.

Lin, Y.P., Singer, P.C., 2006. Inhibition of calcite precipitation by ortho-phosphate: speciation and thermodynamics considerations. Geochimica et Cosmochimica Acta 70 (2006), 2530–2539.

Liu, Y., Tay, J.-H., 2004. State of the art of biogranulation technology for wastewater treatment. Biotechnology Advances 22 (7), 533–563.

Mullen, J.W., (2001). Solutions and Solubility. Crystallization (4th ed.). pp. 86–34.

Münch, E.V., Barrm, K., 2001. Controlled struvite crystallisation for removing phosphorus from anaerobic digester sidestreams. Water Research 35 (1), 151–159.

Maurer, M., Abramovich, D., Siegrist, H., Gujer, W., 1999. Kinetics of biologically induced phosphorus precipitation in waste-water treatment. Water Research 33 (2), 484–493.

Montastruc, L., Azzaro-Pantel, C., Biscans, B., Cabassud, M., Domenech, S., 2003. A thermochemical approach for calcium phosphate precipitation modelling in a pellet reactor. Chemical Engineering Journal 94 (1), 41–50.

Morgan, H., Wilson, R.M., Elliott, J.C., Dowker, S.E.P., Anderson, P., 2000. Preparation and characterisation of monoclinic hydroxyapatite and its precipitated carbonate apatite intermediate. Biomaterials 21 (6), 617–627.

Morgenroth, E., Sherden, T., van Loosdrecht, M.C.M., Hijnen, J.J., Wilderer, P.A., 1997. Aerobic Granular sludge in a sequencing batch reactor. Water Research 31 (12), 3191–3194.

Mostastruc L. 2003. Modélisation et optimisation d'un réacteur en lit fluidisé de déphosphatation d'effluents aqueux. Ph.D. Thesis at INPT and UPS Toulouse III.

Musvoto, E.V., Wentzel, M.C., Ekama, G.A., 2000. Integrated chemical-physical processes modeling -II. Simulating aeration treatment of anaerobic digester supernatants. Water Research 34 (6), 1868–1880.

Ohlinger, K.N., Young, T.M., Shroeder, E.D., 1998. Predicting struvite formation in digestion. Water Research 32 (12), 3607–3614.

Pambrun, V., 2005. Analyse et modélisation de la nitrification partielle et de la précipitation concomitante du phosphore dans un réacteur à alimentation séquencé. INSA, Toulouse.

Pandolfi, D., Pons, M.N., da Motta, M., 2007. Characterization of PHB storage in activated sludge extended filamentous bacteria by automated colour image analysis. Biotechnology Letters 29, 1263–1269.

Parkhurst, D.L., Thorstenson, D.C., Plummer, L.N., 1980. PHREEQC - A computer program for geochemical calculations. U.S. Geol. Surv. Water Resour. Invest. Rep. 80 (96), 210–219.

Rahman, R.N., Ghaza, F.M., Salleh, A.B., et al., 2006. Biodegradation of hydrocarbon contamination by immobilized bacterial cells. Journal Microbiology 44 (3), 354–359.

Ren, T.-T., Liu, L., Sheng, G.-P., Liu, X.-W., Yu, H.-Q., Zhang, M.-C., Zhu, J.-R., 2008. Calcium spatial distribution in aerobic granules and its effects on granule structure, strength and bioactivity. Water Research 42 (13), 3343–3352.

Saidou, H., Korchef, A., Ben Moussa, S., Ben Amor, M., 2009. Struvite precipitation by the dissolved CO2 degasification technique: impact of the airflow rate and pH. Chemosphere 74 (2), 338–343.

Seckler, M.M., Bruinsma, O.S.L., van Rosmalen, G.M., 1996. Phosphate Removal in fluidized bed I. Identification of physical processes. Water Research 30 (7), 1585–1588.

Shu, L., Schneider, P., Jegatheesan, V., Johnson, J., 2006. An economic evaluation of phosphorus recovery as struvite from digester supernatant. Bioresource Technology 97 (17), 2211–2216.

Skoog, Hoeller, Nieman, 2003. In: de Boeck (Ed.), Principes D'analyse Instrumentale, fifth ed.

Snoeyink, V.L., Jenkins, D., 1980. Water Chemistry. John Wiley and Sons, New York.

Suzuki, K., Tanaka, Y., Kuroda, K., Hanajima, D., Fukumoto, Y., Yasuda, T., 2006. The technology of phosphorus removal and recovery from swine wastewater by struvite crystallization reaction. Bioresource Technology 96 (14), 1544–1550.

van Rensburg, P., Musvoto, E.V., Wentzel, M.C., Ekama, G.A., 2003. Modelling multiple mineral precipitation in anaerobic digester liquor. Water Research 37 (13), 3087.

Wan J. 2009. Interaction entre l'élimination des polluants azotées et la formation des granules aérobies en réacteur biologique séquencé. PhD thesis, INSA (Toulouse).

Wan, J., Sperandio, M., 2009. Possible role of denitrification on aerobic granular sludge formation in sequencing batch reactor. Chemosphere 75 (2), 220–227.

Wan, J., Bessière, Y., Spérandio, M., 2009. Alternating anoxic feast/aerobic famine condition for improving granular sludge formation in sequencing batch airlift reactor at reduced aeration rate. Water Research 43 (20), 5097–5108.

Wang, T., Dorner-Reisel, A., Müller, E., 2004. .Thermogravimetric and thermokinetic investigation of the dehydroxylation of a hydroxyapatite powder. Journal of the European Ceramic Society 24 (4), 693.

Wang, H.L., Yu, G.L., Liu, G.S., Pan, F., 2006. A new way to cultivate aerobic granules in the process of paper-making wastewater in a sequencing batch reactor. Biochemical Engineering 28 (11), 99–103.

Yilmaz, G., Lemaire, R., Keller, J., Yuan, Z., 2007. Simultaneous nitrification, denitrification and phosphorus removal from nutrient-rich Industrial wastewater using granular sludge. Biotechnology and Bioengineering 100 (3), 529–541.

Zhu, Gui-bing, Yong-zhen, Peng, Shu-yun, Wu, Shu-ying, Wang, Shi-wei, Xu, 2007. Simultaneous nitrification and denitrification in step feeding biological nitrogen removal process. Journal of Environmental Sciences 9 (19), 1043–1048.